Research

Plant parasitic cyst nematodes redirect host indole metabolism via NADPH oxidase-mediated ROS to promote infection

Divykriti Chopra[1]*, M. Shamim Hasan[1,2]* (ID), Christiane Matera[1], Oliver Chitambo[1], Badou Mendy[1], Sina-Valerie Mahlitz[1], Ali Ahmad Naz[3] (ID), Shelly Szumski[4], Slawomir Janakowski[5], Miroslaw Sobczak[5] (ID), Axel Mithöfer[6] (ID), Tina Kyndt[7] (ID), Florian M. W. Grundler[1] (ID) and Shahid Siddique[1,4] (ID)

[1]Rheinische Friedrich-Wilhelms-University of Bonn, INRES – Molecular Phytomedicine, Karlrobert-Kreiten-Straße 13, Bonn D-53115, Germany; [2]Department of Plant Pathology, Faculty of Agriculture, Hajee Mohammad Danesh Science and Technology University, Dinajpur 5200, Bangladesh; [3]Department of Plant Breeding, Institute of Crop Science and Resource Conservation, University of Bonn, Bonn D-53115, Germany; [4]Department of Entomology and Nematology, University of California, Davis, One Shields Ave, Davis, CA 95616, USA; [5]Department of Botany, Institute of Biology, Warsaw University of Life Sciences (SGGW), Warsaw, PL-02-787, Poland; [6]Research Group Plant Defense Physiology, Max Plank Institute for Chemical Ecology, Hans-Knöll-Straße 8, Jena D-07745, Germany; [7]Department Biotechnology, Research Group Epigenetics & Defence, Coupure links 653, Gent B-9000, Belgium

Summary

• Reactive oxygen species (ROS) generated in response to infections often activate immune responses in eukaryotes including plants. In plants, ROS are primarily produced by plasma membrane-bound NADPH oxidases called respiratory burst oxidase homologue (Rboh). Surprisingly, Rbohs can also promote the infection of plants by certain pathogens, including plant parasitic cyst nematodes.

• The Arabidopsis genome contains 10 Rboh genes (*RbohA–RbohJ*). Previously, we showed that cyst nematode infection causes a localised ROS burst in roots, mediated primarily by *RbohD* and *RbohF*. We also found that plants deficient in *RbohD* and *RbohF* (*rbohD/F*) exhibit strongly decreased susceptibility to cyst nematodes, suggesting that Rboh-mediated ROS plays a role in promoting infection. However, little information is known of the mechanism by which Rbohs promote cyst nematode infection.

• Here, using detailed genetic and biochemical analyses, we identified WALLS ARE THIN1 (WAT1), an auxin transporter, as a downstream target of Rboh-mediated ROS during parasitic infections. We found that WAT1 is required to modulate the host's indole metabolism, including indole-3-acetic acid levels, in infected cells and that this reprogramming is necessary for successful establishment of the parasite.

• In conclusion, this work clarifies a unique mechanism that enables cyst nematodes to use the host's ROS for their own benefit.

Introduction

The oxidative burst, a rapid and transient release of large amounts of reactive oxygen species (ROS), is an essential eukaryotic mechanism for defence against a broad range of microorganisms (Ha *et al.*, 2005). In plants, plasma membrane-bound NADPH oxidases, designated as Rbohs (for respiratory burst oxidase homologues), are the main source of ROS during pathogen-induced oxidative bursts (Torres *et al.*, 1998, 2002; Daudi *et al.*, 2012). The role of Rboh-produced ROS in activating plant defence has long been known (Torres & Dangl, 2005), but Rbohs also promote the infection of plants by various pathogens (Torres *et al.*, 2002, 2017; Trujillo *et al.*, 2006; Asai & Yoshioka, 2009; Pogány *et al.*, 2009; Proels *et al.*, 2010; Marino *et al.*, 2012). Despite this intriguing contradiction, the mechanisms by

which NADPH oxidases promote pathogen infection remain obscure.

Among several types of plant pathogens, plant parasitic nematodes (PPNs) are one of the most destructive and cause huge losses in crop production annually (Nicol *et al.*, 2011). Most of the damage caused by PPNs is due to a small group of root-infecting sedentary endoparasitic nematodes that includes cyst nematodes and root-knot nematodes. The cyst and root-knot nematode infection process can be divided into two major stages: (1) root invasion and induction of a feeding site; and (2) long-time feeding site maintenance and nutrient acquisition. During the first stage, infective juveniles (termed J2s) invade the plant roots and migrate through different tissue layers to reach the vascular cylinder (Holbein *et al.*, 2019; Marhavý *et al.*, 2019). Once there, cyst nematodes induce the development of a syncytium, whereas root-knot nematodes induce five to seven giant cells, and both types of parasites become sedentary. During the subsequent

*These authors contributed equally to this work.

nutrient acquisition stage, initial feeding sites expand, leading to the formation of hypermetabolic sinks from which nematodes draw their nutrients. The development of these feeding sites is accompanied by profound structural and physiological changes in host plants (Siddique & Grundler, 2015, 2018, Gheysen & Mitchum, 2018; Smant *et al.*, 2018).

Previously, we showed that cyst nematode infection causes a localised ROS burst in Arabidopsis roots, mediated primarily by RbohD and RbohF complexes, with no observable contribution from the other eight members of the *Rboh* gene family. We also found that plants deficient in RbohD and RbohF (*rbohD/F*) exhibit strongly decreased susceptibility to cyst nematodes, suggesting that Rboh-mediated ROS play a role in promoting infection (Siddique *et al.*, 2014). Here, using comparative transcriptomics and functional analyses, we explored the mechanism by which NADPH oxidases promote plant infection by examining the plant response to cyst nematodes and root-knot nematodes. We identified a vacuolar protein, WALLS ARE THIN1 (WAT1), as a downstream target of Rboh-mediated ROS. We found that WAT1 redirects host indole metabolism, including auxin accumulation, in infected cells, therefore promoting infection.

Materials and Methods

Plant material and culture conditions

Seeds of *Arabidopsis thaliana* Columbia-0 (Col-0) and mutant lines *rbohD/F*, *rbohD* (Torres *et al.*, 2002), and *wat1 (*Ranocha *et al.*, 2010*)* were surface sterilised by washing in 70% (v/v) ethanol for 5 min followed by washing with 2% (w/v) sodium hypochlorite for 3 min and rinsing twice with sterile water. Seeds were dried on sterile Whatman filter paper or stored at 4°C before plating. Arabidopsis plants were grown at a constant temperature of 23°C, under long-day conditions with 16 h light and 8 h darkness in Petri dishes containing agar medium supplemented with modified Knop nutrient solutions for cyst nematode infection or Murashige & Skoog (MS) medium for root-knot infection, as described previously (Sijmons *et al.*, 1991). Primers used to genotype the mutant lines are listed in Supporting Information Table S1.

Nematode infection assays

Heterodera schachtii second-stage juveniles (J2) were harvested from monoculture as previously described (Shah *et al.*, 2017). For the cyst nematode infection assay, 60–80 J2s were sterilised with 0.05% (w/v) HgCl$_2$, extensively washed in sterile water, and inoculated onto the surface of an agar Knop medium plate containing two 12-d-old Arabidopsis plants under sterile conditions. For each experiment, 15–20 plants were used per genotype, and experiments were repeated at least three times independently. The numbers of female nematodes per plant were counted at 12 d post inoculation (dpi). The sizes of the female nematodes and syncytia were measured at 14 dpi using a Leica DM2000 (Leica Microsystems, Wetzlar,

Germany) dissecting microscope. The syncytia or female nematodes were outlined, and the area was calculated using LAS software (Leica Microsystems).

Meloidogyne incognita was propagated on glasshouse cultures of tomato (*Solanum lycopersicum* cv Moneymaker) plants. As described previously (Mendy *et al.*, 2017), galls on roots of tomato were cut into smaller pieces of *c.* 1 cm, crushed, and incubated for 3 min in 1.5% (w/v) sodium hypochlorite. Subsequently, the suspension was passed through a series of sieves to separate nematode eggs from root debris, and eggs were collected in a 25-μm mesh sieve. For surface sterilisation, eggs were incubated in a 10% (w/v) sodium hypochlorite for 3 min and washed abundantly with sterile water. The suspension was stored at RT in darkness. Freshly hatched J2s were rinsed in water and incubated for 20 min in 0.5% (w/v) streptomycin-penicillin and 0.1% (w/v) ampicillin–gentamycin solution and for 3 min in 0.1% (v/v) chlorhexidine followed by three washes with liberal amounts of sterile autoclaved water. For infection assays with root-knot nematodes, *c.* 100 sterile J2s of *M. incognita* were inoculated onto the surface of agar MS-Gelrite medium plates containing two 12-d-old Arabidopsis plants, and the number of galls was counted at 21 dpi. For each experiment, 15–20 plants were used per genotype, and experiments were repeated at least three times independently.

Statistical analyses

For each nematode infection assay, 15–20 plants were used per genotype, and experiments were repeated multiple times and at least three times independently. Data were analysed for normal distribution (Gaussian) using a Shapiro–Wilk normality test ($\alpha < 0.05$). Normally distributed data were analysed by either *t*-test (two means; $\alpha < 0.05$) or analysis of variance (ANOVA) (multiple means; $\alpha < 0.05$) using GraphPad PRISM (v.8.3.0). ANOVA was followed by appropriate posthoc tests (e.g. Tukey's honest significant difference (HSD)). A nonparametric test, if appropriate, was performed to analyse the data (Kruskal–Wallis test).

Microarray analysis

At 10 h after inoculation with *H. schachtii* J2s, short root segments containing stylet thrusting nematodes were marked under a stereomicroscope. Movements of stylets indicate that J2s are still in the migration phase. The infected area around the nematode head was then dissected and collected in liquid N$_2$. Care was taken not to collect any tip or lateral root primordia. RNA was extracted using an RNeasy Plant Mini kit (Qiagen, Germany) according to the manufacturer's instructions. The quality and quantity of RNA were analysed using an Agilent Bioanalyzer (Agilent Technologies, USA) and a NanoDrop (Thermo Fisher Scientific, Waltham, MA, USA), respectively. The cDNA synthesis was performed with NuGEN's Applause 3′Amp System (NuGEN, Redwood City, CA, USA) according to the manufacturer's instructions. NuGEN's Encore Biotin Module (NuGEN) was used to fragment the cDNA. Hybridisation, washing and

scanning were performed according to the Affymetrix 30 Gene Chip Expression Analysis Technical Manual (Affymetrix, Santa Clara, CA, USA). Three chips were hybridised for both Col-0 and *rbohD/F* infected samples, with each microarray representing an independent biological replicate. The primary data analysis was performed with the Affymetrix Expression Console v.1 software using the MAS5 algorithm. Affymetrix .CDF and .CEL files were loaded into the Windows program RMAExpress (http://rmaexpress.bmbolstad.com/) for background correction, normalisation (quantile), and summarisation (median polish). After normalisation, the computed robust multichip average (RMA) expression values were exported as a log scale to a text file. Probe set annotations were performed by downloading Affymetrix mapping files matching array element identifiers to AGI loci from the ARBC (http://www.arabidopsis.org). The genes with a fold change > 1.5 and FDR value < 5% were selected for enrichment analysis in Gene Ontology (GO) annotations of the domain 'biological process'. Microarray data for Col-0 plants have been published previously (Mendy *et al.*, 2017).

Light microscopy

Arabidopsis wild-type Col-0 and mutant *rbohD/F* and *wat1* plants were grown and inoculated as described above. Samples consisting of root segments and attached juveniles were collected at 2 and 14 dpi. The samples were fixed and embedded in epoxy resin as described previously (Siddique *et al.*, 2012) and sectioned on a Leica RM2165 microtome (Leica Microsystems). After staining with hot 0.1% (w/v) toluidine blue, the samples were examined under an Olympus AX70 'Provis' (Olympus, Tokyo, Japan) light microscope equipped with an Olympus DC90 digital camera. The obtained images were equalised for similar contrast and brightness using Adobe Photoshop software.

Validation of microarray chip data

To validate the microarray expression data, the top four downregulated genes were selected. The samples were collected in the same manner as for the microarray analysis. RNA was extracted using an RNeasy Plant Mini kit (Qiagen, Germany) according to the manufacturer's instructions. cDNA was synthesised using a High Capacity cDNA Reverse Transcription Kit (4368814; Life Technologies), according to the manufacturer's instructions. The transcript abundance of targeted genes was analysed using the Stepone Plus Real-Time PCR System (Applied Biosystems, Waltham, MA, USA). Each sample contained 10 μl of Fast SYBR Green qPCR Master Mix with uracil-DNA, glycosylase and 6-carboxy-X-rhodamine (Invitrogen, Waltham, MA, USA); 0.5 μl of forward primer; 0.5 μl of reverse primer (10 μM); 1 μl of cDNA; and water in 20 μl of total reaction volume. Samples were analysed in three technical replicates. *18S* and *ACT2* genes were used as internal controls. Relative expression was calculated as described previously (Pfaffl, 2001) by which the expression of the target gene was normalised to *18S* to calculate fold change. All primer sequences are listed in Table S1.

Salicylic acid (SA), jasmonic acid (JA), and abscisic acid (ABA) quantification

At 3 d after inoculation with *H. schachtii*, short root segments containing sedentary nematodes and their associated syncytia were marked. The infected region around the nematode was then dissected, collected in liquid N_2, homogenised, and stored at −80°C. Care was taken not to collect any tip or lateral root primordia. Corresponding root segments (excluding root tips and lateral root primordia) from uninfected plants were collected as a control. The material was homogenised using liquid N_2 and extracted at −80°C using the modified Bieleski solvent (Van Meulebroek *et al.*, 2012). After filtration and evaporation, chromatographic separation was performed on a U-HPLC system (Thermo Fisher Scientific) equipped with a Nucleodur C18 column (50 × 2 mm; 1.8 μm) and using a mobile phase gradient consisting of acidified methanol and water. Mass spectrometry analysis was conducted in selected-ion monitoring (SIM) mode with a Q Exactive Orbitrap mass spectrometer (Thermo Fisher Scientific), operating in both positive and negative electrospray ionisation mode at a resolution of 70 000 full width at half maximum (Yimer *et al.*, 2018).

Indole acetic acid (IAA) quantification

At 3 d after inoculation with *H. schachtii*, short root segments containing sedentary nematodes and their associated syncytia were marked. The infected region around the nematode was then dissected, collected in liquid N_2, homogenised, and stored at −80°C. Care was taken not to collect any tip or lateral root primordia. Corresponding root segments (excluding root tips and lateral root primordia) from uninfected plants were collected as a control. IAA was quantified according to Nakamura *et al.* (2013) with the only difference that D5-IAA was used as an internal standard.

Constructs and stable plant transformants

The previously described binary vector *pmdc162-proWAT1:GUS* was used to create stably transformed *pWAT1:GUS* (Col-0 and *rbohD/F*) lines by floral dipping (Clough & Bent, 1998). Transformed seeds were selected on MS medium containing 25 μg ml^{-1} hygromycin. Three independent homozygous lines were selected for further analysis. Three *WAT1* promoter fragments (sequence in Fig. S10, see later) were synthesised by Genewiz LLC and cloned into pDONR207 (Invitrogen). These fragments were then transferred into *pmdc162* (Curtis & Grossniklaus, 2003) by LR reaction. *pmdc162pWAT1^{ROS1}:GUS*, *pmdc162pWAT1^{ROS2}:GUS*, and *pmdc162WAT1^{ros1}:GUS* were introduced into *Agrobacterium tumefaciens* strain GV3101 for floral-dip transformation of Arabidopsis (ecotype Col-0). Seeds were selected on Knop medium containing 25 μg ml^{-1} hygromycin. To generate *pWAT1-n:WAT1*, the *WAT1* coding sequence with *MauBI* and *AscI* restriction sites was synthesised in PUC57 by Genewiz LLC. Then, *GUS* in *pmdc162* was replaced by the *WAT1* coding sequence by classical cloning with the help

of double digestion with *Mau*BI and *Asc*I restriction enzymes (Thermo Scientific, USA), therefore creating the vector *35S: WAT1*. The *35S* promoter was then replaced by three promoter fragments, therefore creating *pWAT1^{ROS1}*, *pWAT1^{ROS2}:WAT1*, and *pWAT1^{ros1}:WAT1*. Constructs were introduced into *A. tumefaciens* strain GV3101 for floral-dip transformation of the Arabidopsis *wat1* mutant background. Seeds were selected on Knop medium containing 25 μg ml^{-1} hygromycin. Three independent homozygous lines were selected for further analysis.

GUS staining

Homozygous lines were grown in Knop or MS medium and infected with cyst or root-knot J2s nematodes to visualise the GUS expression in a time-course analysis. The infected or uninfected roots were incubated with X-gluc for 3–4 h at 37°C. After incubation, the reaction was stopped and samples were washed with 70% (v/v) ethanol. Staining was done at three different time points: 1, 3 and 5 dpi. The GUS-stained syncytia and galls were photographed with a Leica DM8.0 inverted microscope equipped with a Leica DMC4500 digital camera and LAS software (Leica Microsystems). Images were resized, cropped and adjusted for similar brightness, contrast and background using Adobe PHOTOSHOP software.

Results

RbohD and RbohF promote parasitism in cyst nematodes but not root-knot nematodes

We were concerned that the reduction in the number of female cyst nematodes in *rbohD/F* might be due to autoactivation of immune responses in these mutants under our experimental conditions. To rule this out, we tested *rbohD/F* plants with the root-knot nematode *Meloidogyne incognita* as well as with the cyst nematode *Heterodera schachtii*. We grew plants in agar medium, and when the roots had spread throughout the medium, we inoculated plants with cyst or root-knot nematodes. As previously observed (Siddique *et al.*, 2014), *rbohD/F* plants showed an 80% reduction in the number of female cyst nematodes at 14 dpi compared with wild-type plants (Col-0) (Fig. 1a). Average sizes of adult cyst nematode females and their syncytia were also significantly reduced in *rbohD/F* compared with Col-0 (Fig. 1b,c). However, *rbohD/F* plants were significantly more susceptible to root-knot nematodes compared with Col-0 as measured by the number of galls (Fig. 1d; Teixeira *et al.*, 2016). The average diameter of the gall did not differ significantly between Col-0 and *rbohD/F*. These data suggest that RbohD and RbohF play a role in promoting plant susceptibility to cyst nematodes but not to root-knot nematodes.

RbohD and RbohF influence indole metabolism to promote cyst nematode parasitism

To identify target genes acting downstream of ROS that promote cyst nematode infection, we cut hundreds of tiny root segments

(0.1 cm) and performed a comparative transcriptomic study (Fig. S1) between Col-0 and *rbohD/F* infected plants at 10 h after cyst nematode inoculation (hai). This time point reflects the initial stages of nematode infection as concluded from an earlier study (Kammerhofer *et al.*, 2015). Total RNA was extracted, labelled and amplified to hybridise with the GeneChip Arabidopsis ATH1 Genome (Affymetrix UK Ltd). The ATH1 Genome Array contains more than 22 500 probe sets representing *c.* 24 000 genes. Our results indicated that *c.* 6000 genes were differentially regulated (fold change > 2.0 and FDR value < 5%) between Col-0 and *rbohD/F* infected root segments (Table S2). The functional categories that were particularly over-represented among differentially regulated genes include 'response to oxygen containing compound' and 'response to stimulus' (Fig. S2). A striking feature of the transcriptome analysis included a strong decrease in transcript abundance for genes involved in indole metabolic pathways including auxin (IAA) biosynthesis, transport and signalling genes in *rbohD/F* compared with Col-0 after infection (Fig. 2a; Table S3). These results were validated by quantitative RT-PCR (Fig. S3).

To further explore these results, we cut hundreds of microscopic root segments infected by cyst nematodes at 3 dpi and compared the levels of four different hormones (salicylic acid, SA; jasmonic acid, JA; auxin, IAA; abscisic acid, ABA) between Col-0 and *rbohD/F*. We did not see any change in the levels of SA and ABA upon nematode infection (Fig. 2b,c). In comparison with SA and ABA, there was a significant increase in levels of IAA and JA upon infection (Fig. 2d,e). However, increase in JA levels did not differ between Col-0 and *rbohD/F* (Fig. 2e). Notably, IAA was significantly elevated in infected Col-0 roots, whereas it remained at a similar level in control and infected *rbohD/F* roots compared with Col-0 roots (Fig. 2d).

Cyst nematodes fail to activate WAT1 in the absence of RbohD and RbohF

The gene that was most severely downregulated in *rbohD/F* plants relative to the wild-type in our transcriptome analysis (fold change = −38.85) was *WALLS ARE THIN1* (*WAT1*), which encodes a vacuolar auxin transporter. WAT1 is a homologue of *Medicago truncatula Nodulin 21* (*MtN21*), which encodes a plant-specific integral membrane protein that is a member of the plant drug/metabolite exporter (P-DME) family (Ranocha *et al.*, 2013). Although WAT1 has been detected in plasma membrane and vacuole fractions in two independent studies, recent analysis with the pro35S:WAT1-GFP construct demonstrated that WAT1 only localises to the tonoplast (Ranocha *et al.*, 2010). The loss-of-function mutant of *WAT1* confers broad-spectrum resistance to vascular pathogens including the bacteria *Ralstonia solanacearum* and *Xanthomonas campestris* as well as the fungi *Verticillium dahliae* and *V. albo-atrum*. A detailed transcriptomic and metabolomics analyses suggested a general repression of indole metabolism in *wat1* (Ranocha *et al.*, 2010, 2013; Denancé *et al.*, 2013), including a strong decrease in transcript abundance for genes encoding the indole glucosinolate biosynthetic pathway,
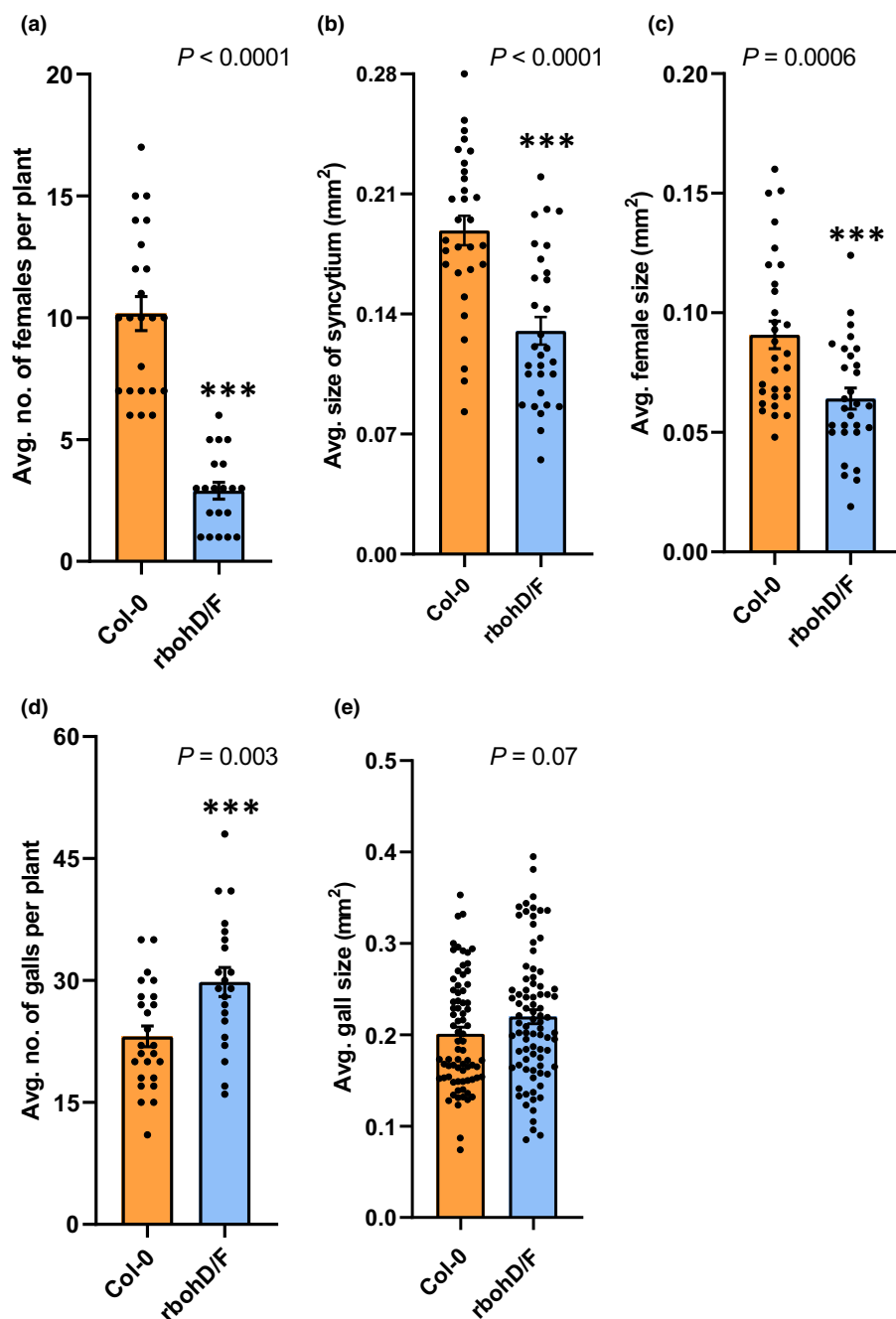
Fig. 1 RbohD and RbohF promote parasitism in beet cyst nematode *Heterodera schachtii* but not root-knot nematode *Meloidogyne incognita*. (a) Average number of female cyst nematodes present per plant root system at 14 d post inoculation (dpi). (b) Average size of plant syncytia at 14 dpi. (c) Average size of female nematodes at 14 dpi. (d) Average number of galls present per plant root system at 20 dpi. (e) Average size of galls at 21 dpi. (a–d) Experiments were performed at least three times independently with the same outcome. Data from one experiment are shown. Bars represent mean ± SE. Data were analysed using *t*-test. Asterisks indicate significant differences compared with Col-0 ($P < 0.05$).

and reduced amounts of indole metabolites such as tryptophan, IAA and IGS.

Similar to analyses of *wat1*, our transcriptomic and hormone analyses of *rbohD/F* roots showed a general repression of indole metabolism, including no increase in IAA levels upon cyst nematode infection. This similarity in mutant phenotypes is consistent with *WAT1* functioning downstream of *RbohD/F* and prompted us to investigate the involvement of WAT1 in cyst nematode infection. First of all, we investigated whether WAT1 and RbohD regulate expression of a common set of genes. To that end, we compared a set of 225 genes that are differentially expressed in *wat1* (Ranocha *et al.*, 2010) with a set of

differentially regulated genes in *rbohD/F*. We found that 75 out of the 225 genes were commonly differentially expressed in *rbohD/F* and *wat1*. Notably, some of these genes encode proteins that play a role in cell wall, auxin, and ethylene metabolism (Table S4).

Next, we assessed *WAT1* gene expression during different stages of nematode infection by evaluating its expression in previously published transcriptomic data (Jammes *et al.*, 2005; Szakasits *et al.*, 2009; Barcala *et al.*, 2010; Mendy *et al.*, 2017). We found that *WAT1* expression was significantly decreased in the syncytium induced by *H. schachtii* at 5 and 15 dpi (Szakasits *et al.*, 2009). However, there was no significant difference in *WAT1*
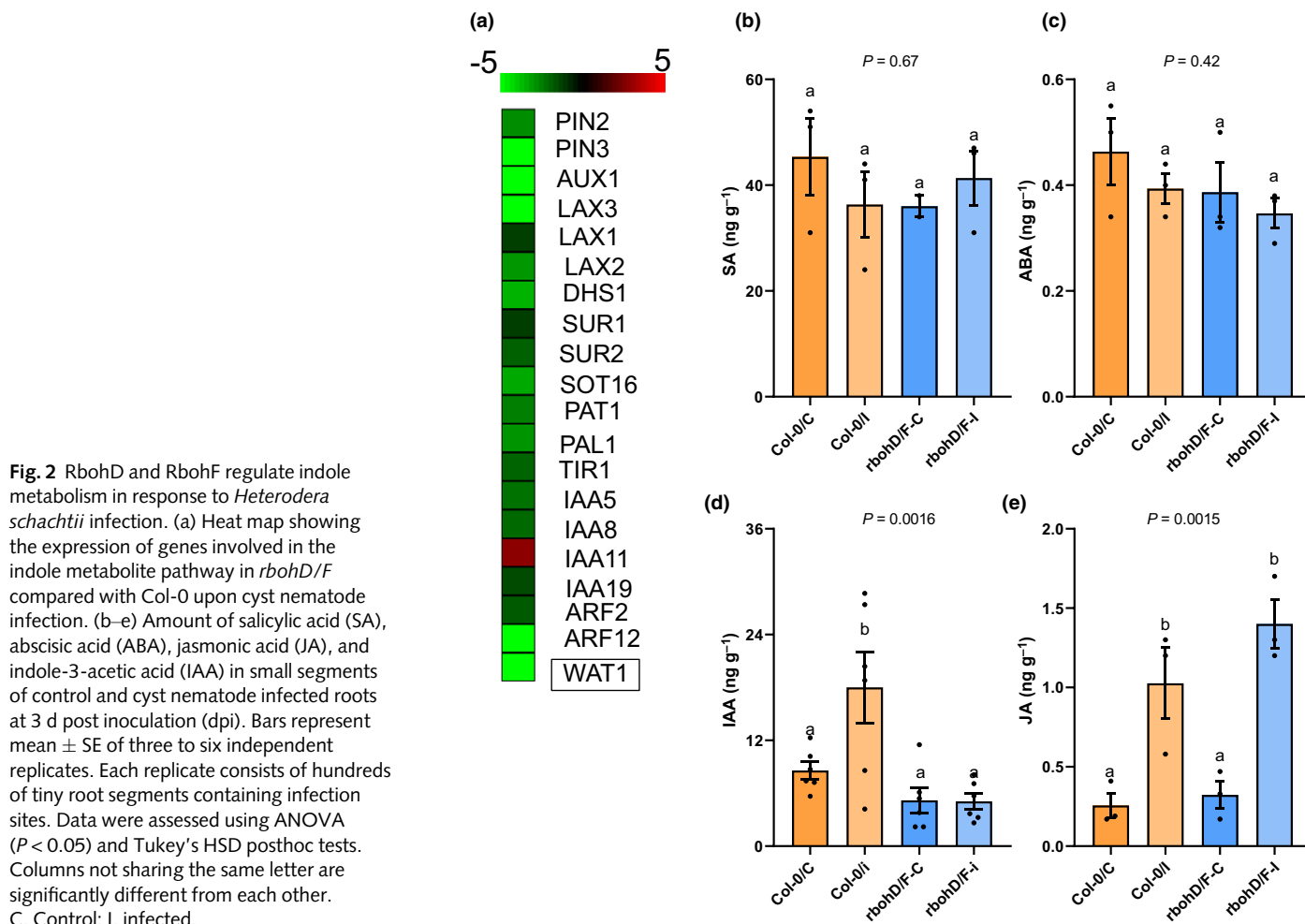
Fig. 2 RbohD and RbohF regulate indole metabolism in response to *Heterodera schachtii* infection. (a) Heat map showing the expression of genes involved in the indole metabolite pathway in *rbohD/F* compared with Col-0 upon cyst nematode infection. (b–e) Amount of salicylic acid (SA), abscisic acid (ABA), jasmonic acid (JA), and indole-3-acetic acid (IAA) in small segments of control and cyst nematode infected roots at 3 d post inoculation (dpi). Bars represent mean ± SE of three to six independent replicates. Each replicate consists of hundreds of tiny root segments containing infection sites. Data were assessed using ANOVA ($P < 0.05$) and Tukey's HSD posthoc tests. Columns not sharing the same letter are significantly different from each other. C, Control; I, infected.

expression levels in root segments containing giant cells or galls infected with the RKN.

To get a detailed insights into the spatio-temporal expression pattern of *WAT1* upon cyst and root-knot nematode infection, we used a reporter line containing the *WAT1* promoter (2980-bp region upstream of the coding sequence) driving GUS gene expression (*pWAT1:GUS*; Ranocha *et al.*, 2010). In general, we did not observe GUS staining in uninfected roots of both Col-0 and *rbohD/F* plants except for a slight background expression that was restricted to younger root zones close to the tips (Ranocha *et al.*, 2010; Fig. S4). by contrast with the uninfected root, most infection zones (*c.* 75%) in infected roots exhibited a strong and specific GUS expression at 1 dpi (Fig. 3a,b). A similar strong GUS expression was detected at 3 and 5 dpi. However, some infection zones showing expression declined as the infection proceeded from 3 dpi onwards (Fig. 3b,c,g,h,i). This expression pattern coincided with the Rboh-mediated ROS production described earlier (Siddique *et al.*, 2014). Markedly, the *pWAT1: GUS* reporter showed either no staining or very low GUS staining in *rbohD/F* lines upon infection by cyst nematodes (Fig. 3d–i). In comparison with cyst nematodes, root-knot nematodes did not induce *pWAT1:GUS* expression during early stages of infection (1 dpi) in Col-0 or *rbohD/F* plants (Fig. S5). However, GUS

expression was occasionally detected in both plant lines at 3 and 5 dpi (Figs S5, S6). To determine if *WAT1* expression is induced by ROS, we incubated *pWAT1:GUS* plants directly in 20 mM H_2O_2 and monitored *GUS* expression after 1 h. Compared with incubation in water, H_2O_2-treated seedlings induced a strong *GUS* expression (Fig. S7). These findings suggested that *WAT1* expression is induced during the initial stages of cyst nematode infection in an Rboh-dependent manner.

WAT1 promotes infection by cyst nematodes but not root-knot nematodes

We examined six genes that are most strongly downregulated in *rbohD/F* compared with Col-0 upon cyst nematode infection and for whose loss-of-function mutants were available (Fig. S8). Of these mutants, only *wat1* plants displayed a significant drop in susceptibility to cyst nematodes relative to Col-0 (Figs 4a, S9). Next, we phenotyped plant roots by measuring the total root length at 12 dpi after counting the nematodes. We found that *wat1* had slightly shorter roots. However, this does not affect the infection phenotype for *wat1*, which still has a significantly reduced number of females per centimetre of root length (Fig. S10). The sizes of syncytia (Fig. 4b) and female nematodes
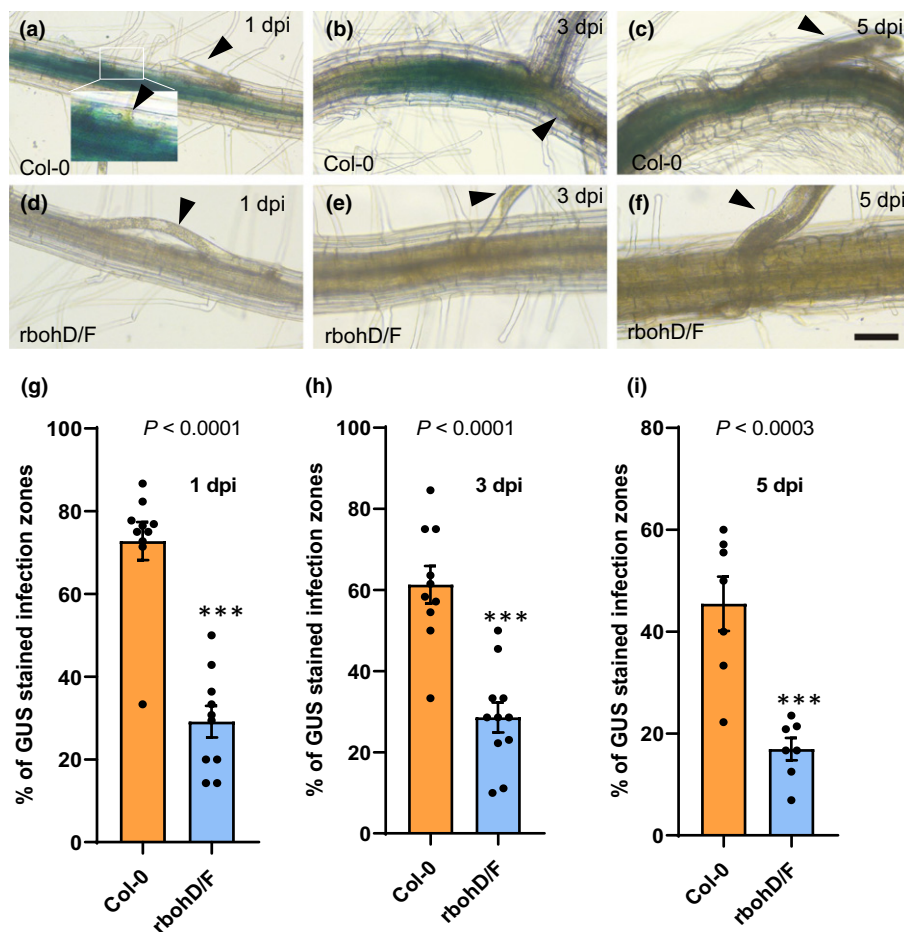
Fig. 3 RbohD and RbohF regulate WAT1 expression in response to *Heterodera schachtii* infection. (a–f) *pWAT1:GUS* expression in Col-0 and *rbohD/F* roots at 1 (a, d), 3 (b, e) and 5 d post inoculation (dpi) (c, f). (g–i) Quantification of *pWAT1:GUS* expression in Col-0 and *rbohD/F* roots upon cyst nematode infection. Bars represent mean ±SE. Three independent experiments were performed, and data are the average for three experiments. Asterisks indicate statistically significant differences with Col-0 using *t*-test (*P* < 0.05). Arrowheads indicate nematodes. Bar, 100 μm.

(Fig. 4c) at 14 dpi were similarly reduced in *wat1* and *rbohD/F* plants compared with Col-0. Upon root-knot nematode infection, the average number of galls increased significantly in *rbohD/F* relative to *wat1* and Col-0 (Fig. 4d). However, there was no difference in infection severity (number and size of galls) between *wat1* and Col-0 (Fig. 4d,e). These data reinforced our view that WAT1 is involved in susceptibility of plants to cyst nematodes.

Because differences in indole metabolism were implicated in nematode susceptibility during our earlier transcriptome analysis and WAT1 is involved in auxin transport, we compared IAA levels between Col-0 and *wat1*. Upon infection with cyst nematodes, IAA accumulated at 3 dpi in Col-0 (Fig. 4f). However, IAA levels were consistently low in *wat1* plants with and without infection. Overall, these results suggested that Rboh-mediated ROS specifically promote cyst nematode infection through *WAT1's* IAA modulating activity (Fig. 4f).

Microscopic examinations of infection showed that in Col-0 roots, most of the juveniles had established well developed syncytia at 2 dpi, and only few vascular cylinder cells were destroyed during nematode migration (Fig. 5). By contrast, nematode invasion caused substantial destruction in the vascular cylinders of *wat1* and *rbohD/F* plants (Fig. 5). Consequently, most of the juveniles had not yet established syncytium in *wat1* and *rbohD/F* at 2 dpi. At 14 dpi, syncytium induced in *wat1* and *rbohD/F* contained fewer incorporated cells, which were less hypertrophied

than elements forming syncytium in infected Col-0 roots. Additionally, both mutants showed fewer cell divisions contributing to the secondary cover tissue (periderm) surrounding the syncytium.

ROS motifs in the WAT1 promoter are required for activation

Our data showed that *WAT1* is regulated by H_2O_2 and RbohD/F during cyst nematode infection, but the regulatory components that activate *WAT1* expression are not known. To identify *cis*-regulatory elements of this gene, we mined the 2980 bp upstream of the *WAT1* coding sequence for the various ROS-responsive motifs as predicted previously (Petrov *et al.*, 2012) and found 19 motifs in this promoter region (Fig. 6a). We split the *WAT1* promoter region into three fragments each containing the TATA box, but a different number of predicted ROS-inducible motifs (Fig. S11): fragment 1 had five ROS-inducible motifs ($pWAT^{ROS1}$); fragment 2 had no ROS-inducible motif ($pWAT^{ros1}$); and fragment 3 had 14 ROS-specific motifs ($pWAT^{ROS2}$). We created stably transformed Arabidopsis lines containing GUS fusion constructs for these three promoter fragments in the Col-0 background and examined GUS expression. In uninfected roots, we did not detect any GUS expression in any of the three lines (Fig. S12), however when infected with cyst nematodes,
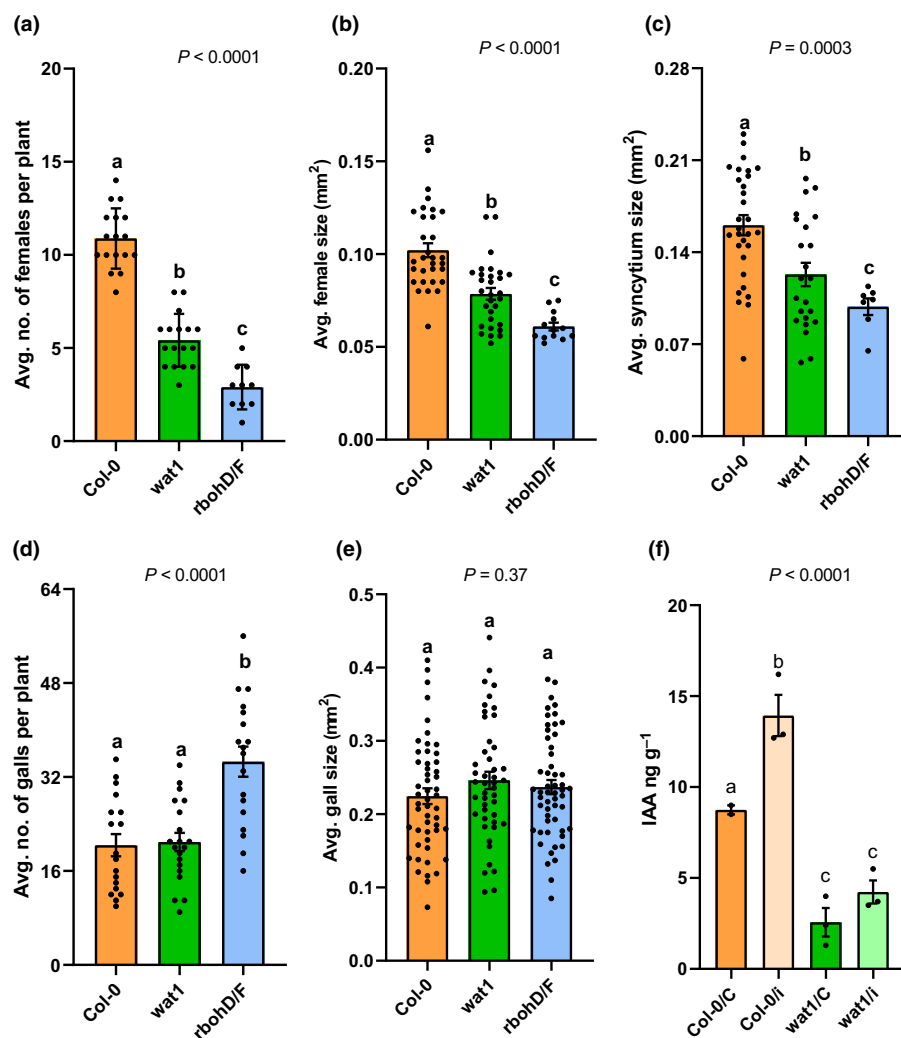
Fig. 4 WAT1 is required for *Heterodera schachtii* infection. (a) Average number of female cyst nematodes present per plant root system at 14 d post inoculation (dpi). (b) Average size of female nematodes at 14 dpi. (c) Average size of plant syncytia at 14 dpi. (d) Average number of galls present per plant root system at 20 dpi. (e) Average size of galls at 21 dpi. (f) Amount of IAA in control and cyst nematode infected roots at 3 dpi measured by UPLC. (a–d) Experiments were performed three to four times independently with the same outcome. Data from one experiment are shown. (e, f) Mean ± SE for four independent biological replicates. Bars represent mean ± SE. Data were assessed using single-factor analysis of variance (ANOVA, $P < 0.05$) and Tukey's HSD posthoc tests. Bars not sharing the same letter are significantly different from each other.
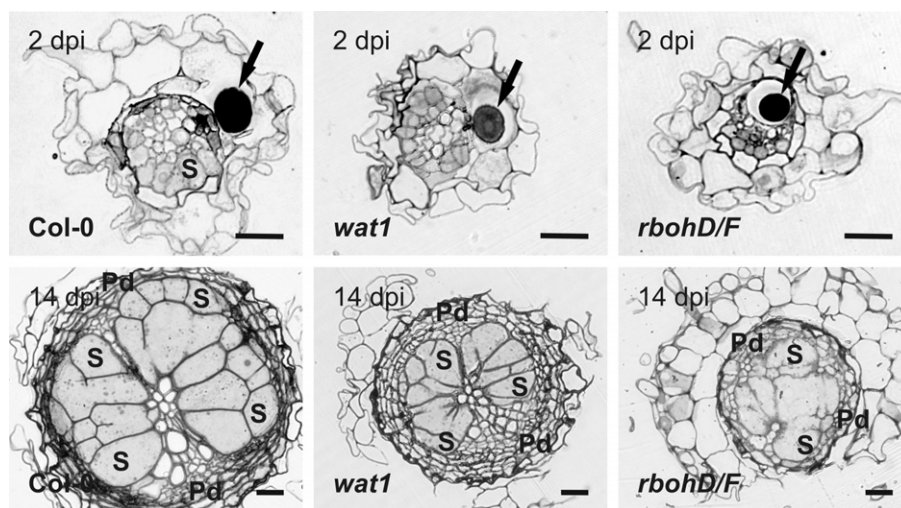

Fig. 5 Cross-sections of *Heterodera schachtii-infected* root sections from Col-0, *wat1-1* and *rbohD/F* at 2 and 14 d post inoculation (dpi). Arrows indicate nematode juveniles. Pd, periderm; S, syncytium. Bars, 20 µm.

$pWAT^{ROS1}:GUS$ and $pWAT^{ROS2}:GUS$ showed GUS expression similar to that observed in $pWAT1:GUS$. Occurrence of GUS staining was reduced strongly for $pWAT^{ros1}:GUS$ upon cyst nematode infection at all three time points (Figs 6, 7). A similar GUS expression pattern was observed in all three lines upon H_2O_2 treatment (Fig. S12). In comparison with cyst nematodes, all three
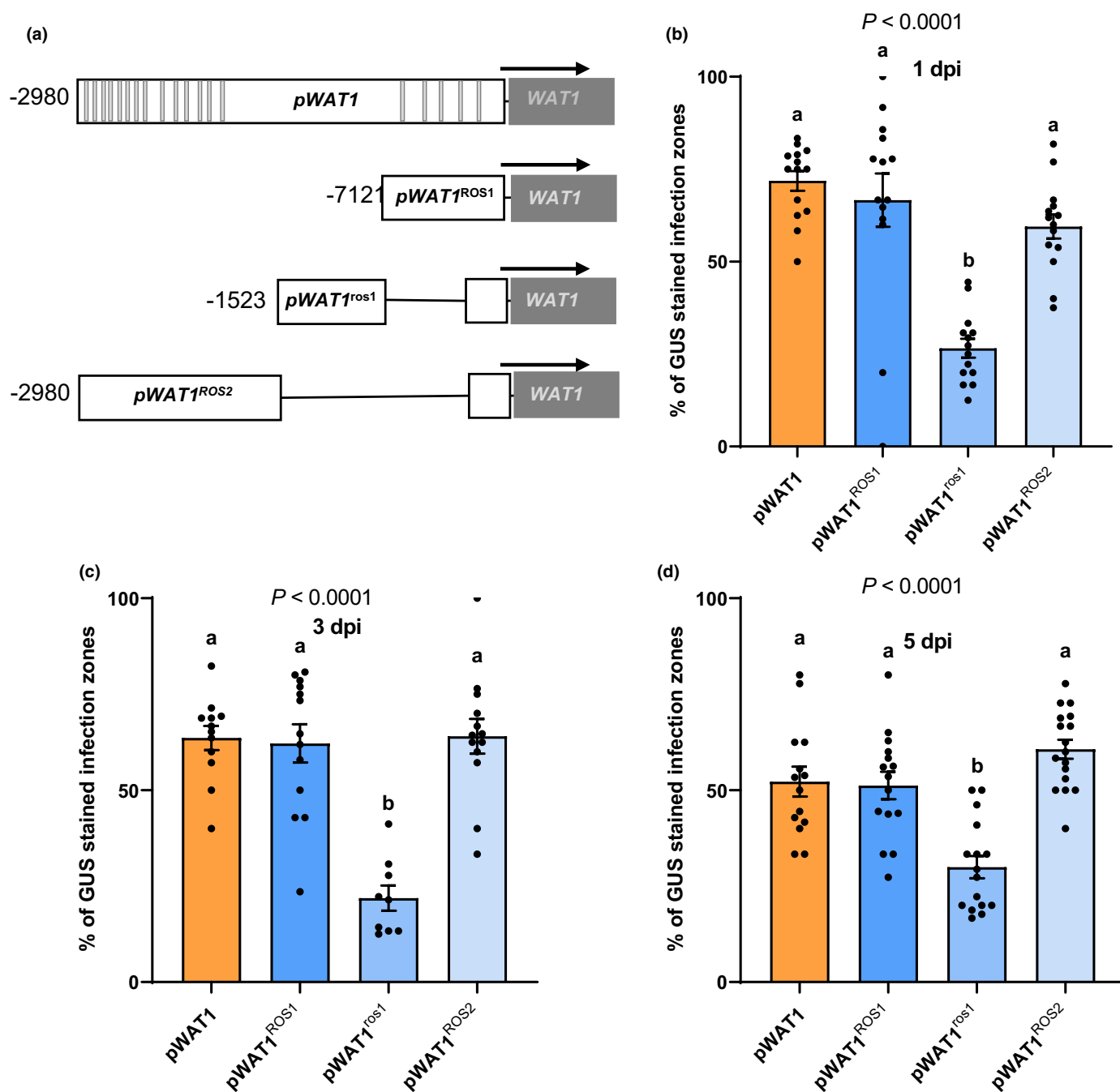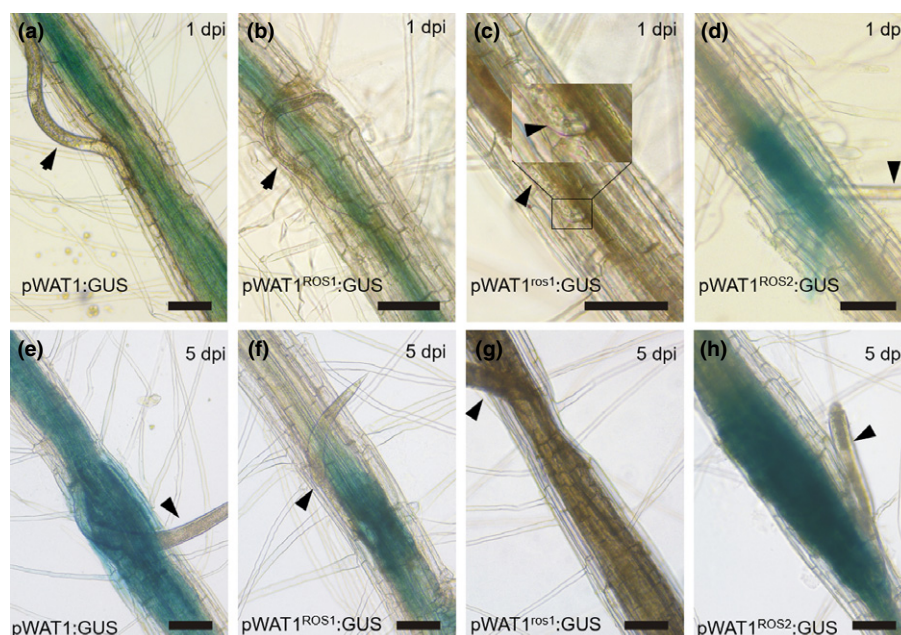
Fig. 6 *Heterodera schachtii* activates the *WAT1* promoter containing ROS-responsive motifs. (a) The *WAT1* promoter was split into three fragments, *pWAT*[ROS1] with five ROS motifs, *pWAT1*[ROS2] with 14 ROS motifs, and *pWAT1*[ros1] with none. (b–d) Quantification of GUS expression driven by various promoter fragments in Col-0 roots upon cyst nematode infection. Bars represent mean ± SE obtained from three independent experiments. Data were subjected to ANOVA ($P < 0.05$) and Tukey's HSD posthoc analysis. Columns not sharing the same letter are significantly different from each other. dpi, days post inoculation.

lines showed occasional GUS expression upon RKN infection that was similar to that observed in *pWAT1:GUS* (Fig. S6).

Next, we tested whether expressing the *WAT1* gene under the control of any of the three promoter fragments (*pWAT*[ROS1]*: WAT1*, *pWAT1*[ROS2]*:WAT1*, and *pWAT1*[ros1]*:WAT1*) could restore susceptibility of *wat1* to wild-type levels. We created stably transformed Arabidopsis lines driving the *WAT1* expression fusion

constructs for these three promoter fragments in the *wat1* background and performed nematode infection assays. We found that *pWAT*[ROS1]*:WAT1* or *pWAT*[ROS2]*:WAT1* restored *wat1* cyst nematode susceptibility to Col-0 levels, whereas *pWAT*[ros1]*:WAT1* did not (Fig. 8a–c). These data suggested that promoter fragments with the presence of ROS-responsive motifs activates *WAT1* expression upon cyst nematode infection.

Fig. 7 *Heterodera schachtii* activates the *WAT1* promoter. (a–h) GUS expression driven by promoter fragments as described in Fig. 6 in transformed Col-0 roots upon cyst nematode infection. Arrowheads point to nematodes. Bars, 100 μm. dpi, days post inoculation.

Constitutive *WAT1* expression rescues the *rbohD* phenotype

We hypothesised that constitutive expression of *WAT1* might increase the susceptibility of *rbohD/F* to cyst nematodes. After several unsuccessful attempts to produce *rbohD/F* mutants with *35S:WAT1*, we continued with the single *rbohD* mutant. We selected two homozygous transgenic *rbohD* lines constitutively expressing *WAT1* (*35S:WAT1/rbohD-L1* and *35S:WAT1/rbohD-L2*; Fig. S13) for further experiments. We did not observe any phenotypic differences between the transgenic lines and Col-0 controls, yet the average number of female nematodes developing on *35S:WAT1/rbohD-L1* and *35S:WAT1/rbohD-L2* was higher than the number found on *rbohD* plants (Fig. 8d). However, the number of nematodes on the rescued lines was still lower than on Col-0, indicating a partial rescue of susceptibility. Furthermore, the average sizes of female nematodes and syncytia increased considerably for individuals developed on *35S:WAT1/rbohD-L1* and *35S:WAT1/rbohD-L2* compared with those found on *rbohD* lines, although they did not attain levels observed on wild-type plants (Fig. 8e,f). Taken together, these data reinforced the view that WAT1 acts downstream of RbohD/F and plays an important in development and functioning of syncytium.

Discussion

In this study, we identified WAT1 as an essential component of the molecular mechanisms underlying RbohD/F-mediated susceptibility to cyst nematodes in plants. We first analysed the expression of *WAT1* in response to cyst and root-knot nematode infection and found commonalities, but also differences. We found that cyst nematode infection induced the localised expression of *WAT1* in roots, which was strongly dependent on *RbohD/F*. This expression was particularly strong during the initial stages of infection suggesting a role for *WAT1* in syncytium initiation

and establishment. Indeed, the reduced number of females, and the smaller size of females and syncytia in *wat1* plants underscored the importance of *WAT1* expression in cyst nematode parasitism. In comparison with cyst nematodes, we did not observe *WAT1* induction during the early stages of root-knot nematode infection. However, GUS expression was occasionally detected in both Col-0 and *rbohD/F* lines at 3 and 5dpi.

Root-knot nematode infection of *rbohD/F* produced an increase in the average number of galls relative to Col-0 (Teixeira *et al.*, 2016), corroborating a previously demonstrated antimicrobial role for Rboh-mediated ROS, but contrasting with our finding that Rbohs play a role in promoting susceptibility to cyst nematodes. However, this dual role of Rbohs can be explained by differences in *WAT1* expression. While infection by cyst nematodes triggered a consistent increase in *WAT1* expression, infection by root-knot nematodes failed to do so. In line with these observations, *wat1* plants showed no change in susceptibility to root-knot nematode infection. We speculated that the difference in *WAT1* expression is likely to be due to a spatio-temporal difference in the ROS production upon cyst nematode versus root-knot nematode infection. A more detailed study will be needed to investigate the changes in ROS production during different stages of cyst and root-knot nematode infection.

Previous transcriptomic and metabolomics analyses suggested a general repression of indole metabolism in *wat1* (Ranocha *et al.*, 2010, 2013; Denancé *et al.*, 2013), which may explain the plethora of phenotypes in *wat1* mutants. Resistance to pathogens is mediated by an increase in SA contents, whereas decreased tryptophan/IAA content is responsible for reduced thickness of stem fibres cell walls. We propose that the Rboh-mediated increase in *WAT1* expression is essential for optimal channelling of indole metabolites, including tryptophan and IAA, in infected cells. This reprogramming of indole metabolites is imperative for the formation and functioning of syncytia. In the absence of ROS in the *rbohD/F* mutant, *WAT1* expression is severely
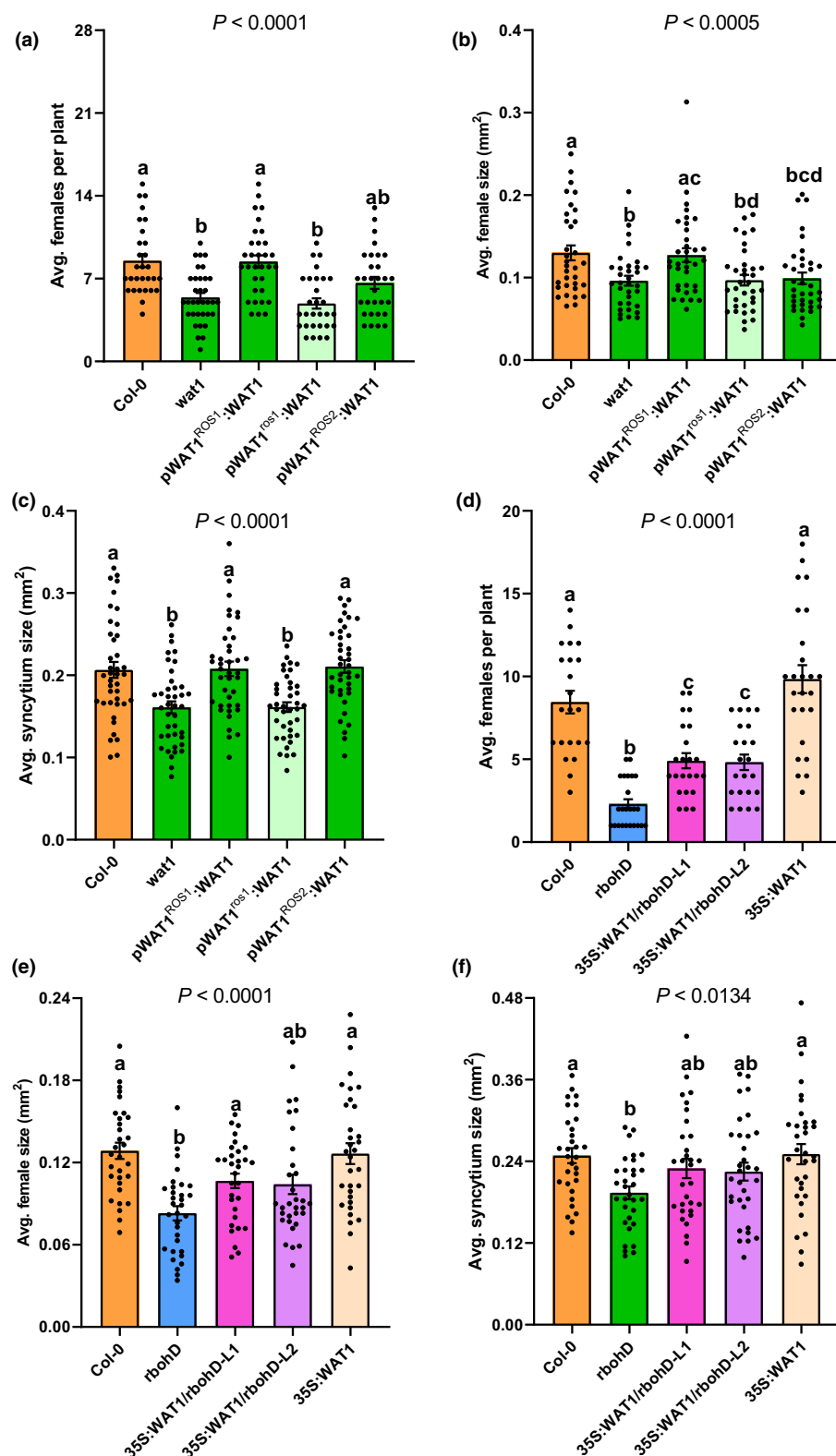
Fig. 8 Minimum ROS motif promoter in the *wat1* mutant and constitutive expression of *WAT1* in *rbohD* mutant restore susceptibility to *Heterodera schachtii*. (a) Average number of female cyst nematodes present in a single root system at 14 d post inoculation (dpi). (b) Average size of female nematodes at 14 dpi. (c) Average size of plant syncytia at 14 dpi. (d) Average number of female cyst nematodes present in a single root system at 14 dpi. (e) Average size of female nematodes at 14 dpi. (f) Average size of plant syncytia at 14 dpi. Bars represent mean ± SE. Data were assessed using single-factor analysis of variance (ANOVA, $P < 0.05$) and Tukey's HSD posthoc tests. Bars not sharing the same letter are significantly different from each other. Experiments were performed three times independently with same outcome. Data from one experiment are shown.

downregulated in an infection-specific manner (Fig. 9). This downregulation of *WAT1* results in the suppression of the indole metabolism causing a failure to induce a feeding site (caused by a lack of IAA accumulation) and poor development of syncytia/nematodes (caused by a lack of IAA accumulation and the

activation of SA responses). Such transport-based modulation of the IAA metabolism has previously been demonstrated for other auxin transporters, such as PIN5 and PIN8, that mediate auxin flow at the ER membrane (Mravec *et al.*, 2009; Ding *et al.*, 2012). As further support for our hypothesis, previous analyses
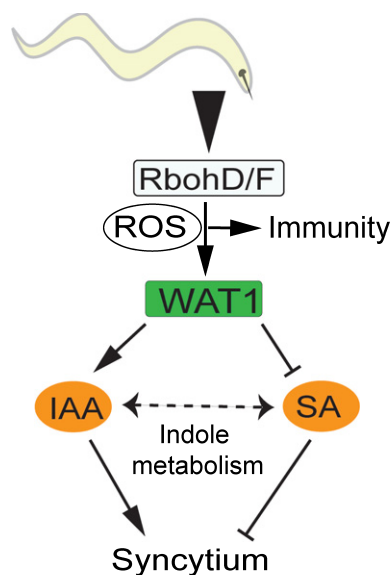
Fig. 9 Scheme of the Rboh-mediated molecular network. *Heterodera schachtii* infection triggers RbohD/F-mediated ROS production, which in turn activates WAT1 and promotes parasite infection by modulating indole metabolism. IAA, indole-3-acetic acid; SA, salicylic acid.

have demonstrated that both SA and auxin are important in the induction and function of syncytia. For example, SA-deficient mutants (*sid2-1*, *pad4-1* and NahG) have been shown to exhibit increased susceptibility to cyst nematodes (Wubben *et al.*, 2008). By contrast, mutants that are deficient in auxin or auxin sig-nalling revealed a significant decrease in susceptibility to both cyst and root-knot nematodes (Goverse *et al.*, 2000; Karczmarek *et al.*, 2004; Grunewald *et al.*, 2009; Kyndt *et al.*, 2016).

The *rboh* mutant plants hyperaccumulate SA, ethylene, and antimicrobial compounds in above-ground tissues upon pathogen challenge (Pogány *et al.*, 2009; Kadota *et al.*, 2014; Torres *et al.*, 2017), leading to the widely accepted belief that accumulation of these compounds is responsible for the reduced susceptibility of *rboh* mutants. However, the mechanism underly-ing accumulation of these compounds in *rbohD/F* remains unknown. One hypothesis is that key plant immune regulators, including Rbohs, are guarded by NLR proteins (nucleotide-binding domain and leucine-rich repeat-containing receptor), that autoactivate immune responses in mutants that are deficient in Rbohs (Kadota *et al.*, 2015). Our data do not support the notion of an NLR-mediated reduction in susceptibility of *rbohD/F* to various pathogens, in particular to cyst nematodes. Instead, they demonstrate a unique role of RbohD/F-mediated ROS as a susceptibility factor in directing host metabolism to promote infection. Our results also establish WAT1 as an essential compo-nent of metabolic pathways linking oxidative burst signals to diverse downstream responses.

Our findings expand the known roles of Rboh in plant growth and immunity (Foreman *et al.*, 2003; Kwak *et al.*, 2003; Miller *et al.*, 2009) by providing details of a unique mechanism that enables parasites to use host NADPH oxidase-mediated ROS for their own benefit. Determining whether nematodes actively release substances (i.e. effectors) to stimulate host ROS

production will be a next step in our emerging understanding of host–parasite interactions.

Author contributions

SSiddique conceptualised the study and acquired the funding. MSH, DC, SV-M, SJ, MS, CM, SSzumski, BM and OC per-formed experiments. MSH, DC, MS, AAN, FMWG and SSid-dique analysed the data. TK and AM performed hormone measurements. DC curated the data and performed the statistics. SSiddique and DC wrote the original draft. All authors con-tributed to editing of manuscript. DC and MSH contributed equally to this work.

ORCID

Florian M. W. Grundler https://orcid.org/0000-0001-8101-0558
M. Shamim Hasan https://orcid.org/0000-0001-6417-9650
Tina Kyndt https://orcid.org/0000-0002-5267-5013
Axel Mithöfer https://orcid.org/0000-0001-5229-6913
Ali Ahmad Naz https://orcid.org/0000-0002-0382-2128
Shahid Siddique https://orcid.org/0000-0001-7503-4318
Miroslaw Sobczak https://orcid.org/0000-0002-4660-6935

Data availability

The paper contain microarray data and it is publicly available through ArrayExpress under accession no. E-MTAB-10625. Raw data for infection assays are provided in Table S5. All transgenic lines are available upon request.

References

Asai S, Yoshioka H. 2009. Nitric oxide as a partner of reactive oxygen species participates in disease resistance to necrotrophic pathogen *Botrytis cinerea* in *Nicotiana benthamiana*. *Molecular Plant–Microbe Interactions* **22**: 619–629.

Barcala M, García A, Cabrera J, Casson S, Lindsey K, Favery B, García-Casado G, Solano R, Fenoll C, Escobar C. 2010. Early transcriptomic events in microdissected Arabidopsis nematode-induced giant cells. *The Plant Journal* **61**: 698–712.

Clough SJ, Bent AF. 1998. Floral dip: a simplified method for Agrobacterium-mediated transformation of *Arabidopsis thaliana*. *The Plant Journal* **16**: 735–743.

Curtis MD, Grossniklaus U. 2003. A Gateway cloning vector set for high-throughput functional analysis of genes in planta. *Plant Physiology* **133**: 462–469.

Daudi A, Cheng Z, O'Brien JA, Mammarella N, Khan S, Ausubel FM, Bolwell GP. 2012. The apoplastic oxidative burst peroxidase in Arabidopsis is a major component of pattern-triggered immunity. *The Plant Cell* 24: 275–287.

Denancé N, Ranocha P, Oria N, Barlet X, Rivière MP, Yadeta KA, Hoffmann L, Perreau F, Clement G, Maria-Grondard A *et al.* 2013. Arabidopsis *wat1* (*walls are thin1)-mediated* resistance to the bacterial vascular pathogen, *Ralstonia solanacearum*, is accompanied by cross-regulation of salicylic acid and tryptophan metabolism. *The Plant Journal* 73: 225–239.

Ding Z, Wang B, Moreno I, Dupláková N, Simon S, Carraro N, Reemmer J, Pěnčík A, Chen Xu, Tejos R *et al.* 2012. ER-localized auxin transporter PIN8 regulates auxin homeostasis and male gametophyte development in Arabidopsis. *Nature Communications* 3: 941.

Foreman J, Demidchik V, Bothwell JHF, Mylona P, Miedema H, Torres MA, Linstead P, Costa S, Brownlee C, Jones JDG *et al.* 2003. Reactive oxygen species produced by NADPH oxidase regulate plant cell growth. *Nature* 422: 442–446.

Gheysen G, Mitchum MG. 2018. Phytoparasitic nematode control of plant hormone pathways. *Plant Physiology* 179: 1212–1226.

Goverse A, Overmars H, Engelbertink J, Schots A, Bakker J, Helder J. 2000. Both induction and morphogenesis of cyst nematode feeding cells are mediated by auxin. *Molecular Plant–Microbe Interactions* 13: 1121–1129.

Grunewald W, Cannoot B, Friml J, Gheysen G. 2009. Parasitic nematodes modulate PIN-mediated auxin transport to facilitate infection. *PLoS Pathogens* 5: e1000266.

Ha EM, Oh CT, Bae YS, Lee W. 2005. A direct role for dual oxidase in Drosophila gut immunity. *Science* 310: 847–850.

Holbein J, Franke RB, Marhavý P, Fujita S, Górecka M, Sobczak M, Geldner N, Schreiber L, Grundler FMW, Siddique S. 2019. Root endodermal barrier system contributes to defence against plant-parasitic cyst and root-knot nematodes. *The Plant Journal* 100: 221–236.

Jammes F, Lecomte P, de Almeida-Engler J, Bitton F, Martin-Magniette ML, Renou JP, Abad P, Favery B. 2005. Genome-wide expression profiling of the host response to root-knot nematode infection in Arabidopsis. *The Plant Journal* 44: 447–458.

Kadota Y, Shirasu K, Zipfel C. 2015. Regulation of the NADPH Oxidase RBOHD during plant immunity. *Plant and Cell Physiology* 56: 1472–1480.

Kadota Y, Sklenar J, Derbyshire P, Stransfeld L, Asai S, Ntoukakis V, Jones JDG, Shirasu K, Menke F, Jones A *et al.* 2014. Direct regulation of the NADPH oxidase RBOHD by the PRR-associated kinase BIK1 during plant immunity. *Molecular Cell* 54: 43–55.

Kammerhofer N, Radakovic Z, Regis JM, Dobrev P, Vankova R, Grundler FM, Siddique S, Hofmann J, Wieczorek K. 2015. Role of stress-related hormones in plant defense during early infection of the cyst nematode *Heterodera schachtii* in Arabidopsis. *New Phytologist* 207: 778–789.

Karczmarek A, Overmars H, Helder J, Goverse A. 2004. Feeding cell development by cyst and root-knot nematodes involves a similar early, local and transient activation of a specific auxin-inducible promoter element. *Molecular Plant Pathology* 5: 343–346.

Kwak JM, Mori IC, Pei ZM, Leonhardt N, Torres MA, Dangl JL, Bloom RE, Bodde S, Jones JDG, Schroeder JI. 2003. NADPH oxidase *AtrbohD* and *AtrbohF* genes function in ROS-dependent ABA signaling in *Arabidopsis*. *EMBO Journal* 22: 2623–2633.

Kyndt T, Goverse A, Haegeman A, Warmerdam S, Wanjau C, Jahani M, Engler G, de Almeida EJ, Gheysen G. 2016. Redirection of auxin flow in *Arabidopsis thaliana* roots after infection by root-knot nematodes. *Journal of Experimental Botany* 67: 4559–4570.

Marhavý P, Kurenda A, Siddique S, Tendon DV, Zhou F, Holbein J, Shamim MH, Grundler FMW, Farmer E, Geldner N. 2019. Single-cell damage elicits regional, nematode-restricting ethylene responses in roots. *EMBO Journal* 38: e100972.

Marino D, Dunand C, Puppo A, Pauly N. 2012. A burst of plant NADPH oxidases. *Trends in Plant Science* 17: 9–15.

Mendy B, Wang'ombe MW, Radakovic ZS, Holbein J, Ilyas M, Chopra D, Holton N, Zipfel C, Grundler FMW, Siddique S 2017. Arabidopsis leucine-rich repeat receptor-like kinase NILR1 is required for induction of innate immunity to parasitic nematodes. *PLoS Pathogens* 13: e1006284.

Miller G, Schlauch K, Tam R, Cortes D, Torres Ma, Shulaev V, Dangl Jl, Mittler R 2009. The plant NADPH oxidase RBOHD mediates rapid systemic signaling in response to diverse stimuli. *Science Signalling* 2: ra45.

Mravec J, Skůpa P, Bailly A, Hoyerová K, Křeček P, Bielach A, Petrášek J, Zhang J, Gaykova V, Stierhof Y-D *et al.* 2009. Subcellular homeostasis of phytohormone auxin is mediated by the ER-localized PIN5 transporter. *Nature* 459: 1136–1140.

Nakamura Y, Reichelt M, Mayer VE, Mithöfer A. 2013. Jasmonates trigger pre induced formation of 'outer stomach' in carnivorous sundew plants. *Proceedings of the Royal Society B: Biological Sciences* 280: 20130228.

Nicol JM, Turner SJ, Coyne DL, Den Nijs L, Hockland S, Maafi ZT. 2011. Current nematode threats to world agriculture. In: Jones J, Gheysen G, Fenoll C, eds, *Genomics and molecular genetics of plant-nematode interactions*. Dordrecht, the Netherlands: Springer, 21–43.

Petrov V, Vermeirssen V, De Clercq I, Van Breusegem F, Minkov I, Vandepoele K, Gechev TS. 2012. Identification of cis-regulatory elements specific for different types of reactive oxygen species in *Arabidopsis thaliana*. *Gene* 499: 52–60.

Pfaffl MW. 2001. A new mathematical model for relative quantification in real-time RT-PCR. *Nucleic Acids Research* 29: e45.

Pogány M, von Rad U, Grün S, Dongó A, Pintye A, Simoneau P, Bahnweg G, Kiss J, Barna B, Durner J *et al.* 2009. Dual roles of reactive oxygen species and NADPH oxidase RBOHD in an Arabidopsis-*Alternaria* pathosystem. *Plant Physiology* 151: 1459–1475.

Proels RK, Oberhollenzer K, Pathuri IP, Hensel G, Kumlehn J, Hückelhoven R. 2010. RBOHF2 of barley is required for normal development of penetration resistance to the parasitic fungus *Blumeria graminis* f. sp *hordei*. *Molecular Plant–Microbe Interactions* 23: 1143–1150.

Ranocha P, Denancé N, Vanholme R, Freydier A, Martinez Y, Hoffmann L, Kohler L, Pouzet C, Renou J-P, Sundberg B *et al.* 2010. *Walls are thin 1* (*WAT1*), an Arabidopsis homolog of *Medicago truncatula NODULIN21*, is a tonoplast-localized protein required for secondary wall formation in fibers. *The Plant Journal* 63: 469–483.

Ranocha P, Dima O, Nagy R, Felten J, Corratgé-Faillie C, Novák O, Morreel K, Lacombe B, Martinez Y, Pfrunder S *et al.* 2013. Arabidopsis *WAT1* is a vacuolar auxin transport facilitator required for auxin homoeostasis. *Nature Communications* 4: 2625.

Shah SJ, Anjam MS, Mendy B, Anwer MA, Habash SS, Lozano-Torres JL, Grundler FMW, Siddique S. 2017. Damage-associated responses of the host contribute to defence against cyst nematodes but not root-knot nematodes. *Journal of Experimental Botany* 68: 5949–5960.

Siddique S, Grundler FMW. 2015. Metabolism in nematode feeding sites. *Advances in Botanical Research* 73: 119–138.

Siddique S, Grundler FMW. 2018. Parasitic nematodes manipulate plant development to establish feeding sites. *Current Opinion in Microbiology* 46: 102–108.

Siddique S, Matera C, Radakovic Zs, Shamim Hasan M, Gutbrod P, Rozanska E, Sobczak M, Torres MA, Grundler FMW. (2014). Parasitic worms stimulate host NADPH oxidases to produce reactive oxygen species that limit plant cell death and promote infection. *Science Signalling* 7, ra33.

Siddique S, Sobczak M, Tenhaken R, Grundler FMW, Bohlmann H. 2012. Cell wall ingrowths in nematode induced syncytia require UGD2 and UGD3. *PLoS ONE* 7: e41515.

Sijmons PC, Grundler FMW, von Mende N, Burrows PR, Wyss U. 1991. *Arabidopsis thaliana* as a new model host for plant-parasitic nematodes. *The Plant Journal* 1: 245–254.

Smant G, Helder J, Goverse A. 2018. Parallel adaptations and common host cell responses enabling feeding of obligate and facultative plant parasitic nematodes. *The Plant Journal* 93: 686–702.

Szakasits D, Heinen P, Wieczorek K, Hofmann J, Wagner F, Kreil DP, Sykacek P, Grundler FM, Bohlmann H. 2009. The transcriptome of syncytia induced by the cyst nematode *Heterodera schachtii* in Arabidopsis roots. *The Plant Journal* 57: 771–784.

Teixeira MA, Wei L, Kaloshian I. 2016. Root-knot nematodes induce pattern-triggered immunity in *Arabidopsis thaliana* roots. *New Phytologist* 211: 276–287.

Torres DP, Proels RK, Schempp H, Huckelhoven R. 2017. Silencing of *RBOHF2* causes leaf age-dependent accelerated senescence, salicylic acid accumulation, and powdery mildew resistance in barley. *Molecular Plant–Microbe Interactions* 30: 906–918.

Torres MA, Dangl JL, Jones JDG. 2002. Arabidopsis gp91[phox] homologues *AtrbohD* and *AtrbohF* are required for accumulation of reactive oxygen intermediates in the plant defense response. *Proceedings of the National Academy of Sciences, USA* 99: 517–522.

Torres MA, Dangl JL. 2005. Functions of the respiratory burst oxidase in biotic interactions, abiotic stress and development. *Current Opinion in Plant Biology* 8: 397–403.

Torres MA, Onouchi H, Hamada S, Machida C, HammondKosack KE, Jones JD. 1998. Six *Arabidopsis thaliana* homologues of the human respiratory burst oxidase (*gp91[phox]*). *The Plant Journal* 14: 365–370.

Trujillo M, Altschmied M, Schweizer P, Kogel KH, Huckelhoven R. 2006. Respiratory burst oxidase homologue A of barley contributes to penetration by the powdery mildew fungus *Blumeria graminis* f. sp *hordei*. *Journal of Experimental Botany* 57: 3781–3791.

Van Meulebroek L, Bussche JV, Steppe K, Vanhaecke L. 2012. Ultra-high-performance liquid chromatography coupled to high resolution Orbitrap mass spectrometry for metabolomic profiling of the endogenous phytohormonal status of the tomato plant. *Journal of Chromatography A* 1260: 67–80.

Wubben MJE, Jin J, Baum TJ. 2008. Cyst nematode parasitism of *Arabidopsis thaliana* is inhibited by salicylic acid (SA) and elicits uncoupled SA-independent pathogenesis-related gene expression in roots. *Molecular Plant–Microbe Interactions* 21: 424–432.

Yimer HZ, Nahar K, Kyndt T, Haeck A, Van Meulebroek L, Vanhaecke L, Demeestere K, Hofte M, Gheysen G. 2018. Gibberellin antagonizes jasmonate-induced defense against *Meloidogyne graminicola* in rice. *New Phytologist* 218: 646–660.

Supporting Information

Additional Supporting Information may be found online in the Supporting Information section at the end of the article.

Fig. S1 Schematic of microscopic samples for transcriptomic study between Col-0 and *rbohD/F* plants.

Fig. S2 GO enrichment among differentially regulated genes between Col-0 and *rbohD/F* at 10 h post inoculation.

Fig. S3 Validation of transcriptome results.

Fig. S4 *pWAT1:GUS* expression in Col-0 and *rbohD/F* uninfected roots.

Fig. S5 WAT1 expression in response to root-knot nematode infection.

Fig. S6 Analysis of *pWAT1:GUS* expression upon root-knot nematode infection.

Fig. S7 WAT1 induction by H2O2.

Fig. S8 Cyst nematode assays for loss-of-function mutants for six significantly downregulated genes in *rbohD/F* compared with Col-0 upon infection.

Fig. S9 WAT1 is required for cyst nematode infection.

Fig. S10 WAT1 is required for cyst nematode infection.

Fig. S11 Sequence of WAT1 Promoter fragments generated based on the presence or absence of *cis*-regulatory ROS motifs.

Fig. S12 WAT1 induction by H_2O_2.

Fig. S13 Analysis of *WAT1* expression in Col-0, *rbohD*, and *35S: WAT1/rbohD* lines.

Table S1 Primer sequences used in this study.

Table S2 List of differentially regulated genes between Col-0 and rbohD/F at 10 h post inoculation.

Table S3 Expression of genes involved in auxin biosynthesis, transport and signalling in rbohD/F compared with Col-0 10 h post inoculation.

Table S4 List of commonly differentially expressed genes in rbohD/F and wat1.

Table S5 Raw data for infection assays.

Please note: Wiley Blackwell are not responsible for the content or functionality of any Supporting Information supplied by the authors. Any queries (other than missing material) should be directed to the *New Phytologist* Central Office.